Tanshinone IIA regulates the TGF-β1/Smad signaling pathway to ameliorate non-alcoholic steatohepatitis-related fibrosis

LIANJIE XU[1], YURONG ZHANG[1], NENGBO JI[1], YAN DU[1], TAO JIA[2], SHANSHAN WEI[1], WEI WANG[1], SHAN ZHANG[1,3,4*] and WENHUI CHEN[1,3,4*]

[1]Faculty of Basic Medicine, Yunnan University of Traditional Chinese Medicine, Kunming, Yunnan 650500; [2]Department of Orthopedics, First Clinical Medical College of Yunnan University of Traditional Chinese Medicine, Kunming, Yunnan 650021; [3]Yunnan Provincial Key Laboratory of Molecular Biology for Sinomedicine; [4]Key Laboratory of Microcosmic Syndrome Differentiation, Yunnan University of Traditional Chinese Medicine, Kunming, Yunnan 450500, P.R. China

Received February 8, 2022; Accepted May 4, 2022

DOI: 10.3892/etm.2022.11413

Abstract. Tanshinone IIA (TIIA) is a major component extracted from the traditional herbal medicine *Salvia miltiorrhiza* and has been indicated to play a role in the treatment of organ fibrosis. However, the evidence supporting its antifibrotic effect is insufficient and the underlying mechanism is unclear. To investigate the therapeutic effect of TIIA on non-alcoholic steatohepatitis-related fibrosis (NASH-F), the present study used a methionine choline deficiency diet to induce NASH-F in rats, and explored the effect of TIIA on the transforming growth factor-β1 (TGF-β1)/Smad signaling pathway. Wistar rats were randomly divided into control, NASH-F and TIIA groups. After 8 weeks of treatment, the levels of serum markers associated with liver function and fibrosis were measured, liver fat vacuoles and inflammation were assessed by haematoxylin and eosin staining, and liver fibrosis was assessed by Masson's trichrome staining. TGF-β1, Smad2, Smad3, Smad7 and α-smooth muscle actin (α-SMA) mRNA expression, and TGF-β1, Smad2/3, phosphorylated (p)-Smad2/3, Smad7 and α-SMA protein levels were determined. The results revealed that TIIA could remarkably ameliorate liver fat vacuoles and inflammation in NASH-F rats, and could decrease the levels of serum aspartate aminotransferase, alanine aminotransferase, total bilirubin, total bile acid, hyaluronic acid, type IV collagen, laminin and type III collagen, while increasing the levels of total cholesterol and triglycerides; however, this was not statistically significance. TIIA markedly suppressed the increased TGF-β1, Smad2, Smad3 and α-SMA mRNA expression levels observed in the liver of NASH-F rats, while it increased the mRNA expression level of Smad7. Similarly, TIIA suppressed the increased TGF-β1, p-Smad2/3 and α-SMA protein levels observed in the liver of NASH-F rats, while it increased the protein expression level of Smad7 *in vitro* and *in vivo*. TIIA had no significant cytotoxic effect at 10, 20, 40 and 80 μmol/l on human LX-2 cell. In conclusion, the findings of the present study indicated that TIIA alleviated NASH-F by regulating the TGF-β1/Smad signaling pathway. TIIA may be a useful tool in the prevention and treatment of NASH-F.

Introduction

In 2020, the term metabolic dysfunction-associated fatty liver disease (MAFLD) was suggested as a replacement for the term non-alcoholic fatty liver (NAFL) disease for describing a diseased condition of the liver, which is characterized by hepatic steatosis and fat accumulation, and induced by metabolic disorders in addition to alcohol and other factors (1). Currently, the global prevalence of MAFLD is 25%. MAFLD includes pathological features, such as NAFL with or without mild inflammation, non-alcoholic steatohepatitis (NASH) and different degrees of hepatic fibrosis (HF); moreover, severe MAFLD cases may develop into liver cirrhosis and hepatocellular carcinoma (HCC) (2). NASH is a critical subtype of MAFLD, with ~20% of patients with NAFL developing NASH, 10-29% of patients with NASH developing HF or cirrhosis and 4-27% of the latter progressing to developing HCC with cirrhosis (3). NASH-related fibrosis (NASH-F) is the last reversible step before progressing to HCC (4). Therefore, the treatment of NASH-F is an important target in MAFLD therapy.

HF is a multipurpose wound-healing process that is presented as the key early stage of liver cirrhosis. In the

Correspondence to: Dr Shan Zhang or Professor Wenhui Chen, Faculty of Basic Medicine, Yunnan University of Traditional Chinese Medicine, 1076 Yuhua Road, Chenggong, Kunming, Yunnan 650500, P.R. China
E-mail: zhsh0714zs@163.com
E-mail: cwh6581908@126.com

*Contributed equally

Key words: hepatic fibrosis, non-alcoholic steatohepatitis, tanshinone IIA, TGF-β1/Smad

absence of liver transplantation, HF can eventually develop into HCC (5). HF is a complex pathological process, and its exact pathogenesis remains unknown. It is characterized by mass production of extracellular matrix (ECM) by activated hepatic stellate cells (HSCs) that undergo myofibroblast transformation; these activated HSCs can be identified by the expression of α-smooth muscle actin (α-SMA) (6,7). Increasing evidence indicates that the transforming growth factor-β (TGF-β) pathway plays a major role in the development of HF (8,9). The Smad protein family comprises TGF-β downstream signaling molecules, through which TGF-β signals from the cell surface to the nucleus. TGF-β1 mediates the activation and proliferation of HSCs through the classical TGF-β1/Smad2/3 signaling pathway (10). Previous research has demonstrated that TGF-β signaling participates in all stages of liver disease progression, with high TGF-β signaling activity leading to the activation of HSCs, their transdifferentiation to myofibroblasts and the cell death of a large number of hepatocytes, all of which contribute to the development of HF (11). Therefore, targeting the TGF-β pathway appears to be a promising strategy for the treatment of various pathological mechanisms associated with HF (12).

TGF-β is a major pro-fibrotic cytokine that plays a critical role in the development of HF by regulating the activation of HSCs and the mass production of ECM (13,14). Mechanistically, TGF-β1 binds to the TGF-β type I (TGF-βRI) and type II receptors and activates Smad2/3. Subsequently, activated Smad2/3 associates with Smad4, and the complex translocates to the nucleus where it acts as a transcription factor regulating the expression of specific genes (TGF-β canonical pathway) (11). Smad signaling also induces the transcription of fibrosis-related Smad7 target genes; whereas Smad3 is known to promote TGF-β signaling, Smad7 acts as an inhibitor of the pathway (15). Specifically, the Smad7 protein is an inhibitory protein that inhibits TGF-β1 receptor and phosphorylation of its downstream mediators Smad2/3, thereby blocking the TGF-β1 signaling cascade (16). Thus, in the context of HF, Smad7 can attenuate the TGF-β1-mediated activation of HSCs, reduce the expression of pro-fibrotic genes, such as collagen type I and α-SMA, and inhibit the production of ECM, thereby reversing fibrosis (16). The TGF-β1/Smad signaling pathway plays an important role in the occurrence and development of HF, given that TGF-β1 can stimulate the proliferation and activation of HSCs. TGF-β1 signaling is transduced from the plasma membrane to the nucleus through the Smad proteins, where they control laminin (LN) and hyaluronic acid (HA) expression, eventually leading to the occurrence and progression of HF (17,18). Taken together, the TGF-β1/Smad pathway plays an important regulatory role both in development and reversion of HF. Therefore, regulation of the TGF-β1/Smad signaling pathway can be used as an important research target both for preventing and treating NASH-F.

Traditional Chinese Medicine (TCM) and its effective components present great potential in the treatment of fibrosis. For example, Peng *et al* (19) demonstrated that *Salvia miltiorrhiza* treatment could significantly alleviate elevated levels of serum aspartate aminotransferase (AST) and alanine aminotransferase (ALT) and could reduce liver inflammation and fibrosis in a CCl4-induced animal model. Tanshinone IIA (TIIA) is the most abundant lipid-soluble constituent of *Salvia miltiorrhiza Bunge*, and has been widely used in the treatment of cardiovascular diseases (20), atherosclerosis (21) and Alzheimer's disease (22). In recent years, TIIA has also been used for the treatment of visceral fibrosis, including lung, heart, kidney and uterus fibrosis, and it has been demonstrated that TIIA mediates its anti-fibrotic effects through TGF-β/Smad, NF-κB and nuclear factor erythroid 2-related factor 2 (23). Furthermore, Shi *et al* (24) found that TIIA attenuated liver injury, alleviated ECM accumulation, and decreased HSC proliferation and activation in a CCl4-induced rat model of HF, thus exerting potent anti-fibrotic effects. In addition, TIIA has been shown to significantly inhibit the activation of LX-2 induced by TGF-β1 (25). However, the precise underlying molecular mechanism of action of TIIA in hepatic fibrosis remains unknown. Therefore, the present study investigated the potential beneficial effects of TIIA and its underlying mechanism in alleviating liver fibrosis.

Materials and methods

Animals and treatments. Specific pathogen-free 7-week-old 15 male and 15 females Wistar rats (160-200 g) were purchased from the Institute of Medical Biology, Chinese Academy of Medical Sciences [SCXK (Dian) K2019-0002]. Before the start of the experiment, rats were acclimated for 7 days in the facility under standard environmental conditions (23±2˚C; humidity, 60±5%; 12/12 h light/dark cycle with lights on at 8:00 a.m.) and had access to food and water *ad libitum*. All animals received humane care according to institutional animal care guidelines approved by the Experimental Animal Ethics Committee of Yunnan University of Traditional Chinese Medicine (Kunming, China; approval no. R-062021021). The animals were then randomly divided into three groups (n=10 per group): i) Control group, continuously fed standard chow; ii) NASH-F group, fed methionine choline deficiency (MCD) diet; and iii) TIIA group, fed MCD diet and being administered TIIA. The groups were treated with the standard or MCD diet for 8 weeks. Rats in the drug treatment group received TIIA (20 mg/kg/day) via intraperitoneal injection during MCD diet feeding and were weighed daily, while the rats in the other groups were given an equal volume of normal saline via intraperitoneal injection. The doses of TIIA were calculated according to previous research (Liu *et al*, unpublished data) on mice induced by the MCD diet, adjusted to reflect the differences in the body surface area between animals. At the end of the treatment period the rats were anesthetized with 30 mg/kg intraperitoneal sodium pentobarbital injection and sacrificed via cervical dislocation after collection of blood from the abdominal veins of each animal in each group. Serum was collected at 377.325 x g for 10 min at 4˚C by centrifugation and preserved at -80˚C until further analysis. Liver tissues were immediately obtained and fixed in 4% paraformaldehyde for ≥48 h at room temperature.

Reagents. TIIA was purchased from Shanghai Aladdin Biochemical Technology Co., Ltd. (cat. no. H31022558). MCD and standard diet were obtained from Nantong Chem-Base Co., Ltd. (cat. nos. TP3622657 and TP3622647C). AST (cat. no. C0010-2-1), ALT (cat. no. C009-2-1), triglycerides (TG) (cat. no. A110-1-1), total cholesterol (TC) (cat. no. A111-1-1), total bilirubin (TBIL) (cat. no. C019-1) and total bile

acid (TBA) (cat. no. E003-2-1) test kits were purchased from Nanjing Jiancheng Bioengineering Institute. HA, LN, type III collagen (PC-III) and type IV collagen (IV-C) in the rat serum were measured using ELISA assay kits (Meimian Industrial Co., Ltd.). RIPA buffer, PMSF and bicinchoninic acid (BCA) protein concentration kit were purchased from Beyotime Institute of Biotechnology. Antibodies against TGF-β1 (cat. no. Ab215715), Smad2/3 (cat. no. Ab202445), Smad7 (cat. no. Ab272928), α-SMA (cat. no. Ab124964), phosphorylated (p)-Smad2/3 (cat. no. Ab254407) and β-actin (cat. no. Ab8226) were purchased from Abcam, Inc. TRIzol® was purchased from Invitrogen; Thermo Fisher Scientific, Inc. (cat. no. 15596026). ReverTra Ace™ qPCR RT Master Mix with gDNA Remover and SYBR-Green Realtime PCR Master Mix were purchased from Toyobo Life Science. The primer sequences of the target genes were synthesized by Sangon Biotech Co., Ltd. Recombinant human TGF-β1 (cat. no. 100-21-10 μg) was purchased from PeproTech, Inc.

Biochemical parameters. Liver function was evaluated based on the levels of AST, ALT, TBIL and TBA in the rat serum. The kits were used according to the manufacturer's instructions, and the optical density (OD) values for ALT, AST, TC, TG, TBIL and TBA were obtained using a Spark 10M multimode reader (Tecan Group, Ltd.), using the appropriate wavelengths. The concentrations of the aforementioned indicators were calculated using the OD value.

ELISA. HA, IV-C, LN and PC-III in the rat serum were detected using ELISA assay kits according to the manufacturer's instructions. The absorbance was measured using a microplate reader at 450 nm, and the concentrations of the aforementioned indicators were calculated using the OD value.

Histological analysis. Liver tissues were fixed in 4% paraformaldehyde for at least 48 h, dehydrated, embedded in paraffin, and cut into 5-μm thick sections. Liver sections were deparaffinized in xylene for 45 min, rehydrated in a graded alcohol series, then stained with hematoxylin for 3 min and eosin for 30 sec. All steps were carried out at room temperature. For Masson's trichrome staining, the sections were deparaffinized and rehydrated as previously described. Then, sections were stained with hematoxylin, differentiated with acid ethanol, stained in Masson's blue solution, followed by staining with Fuchsin for 8 min. The tissues were then washed with phosphomolybdic acid for 2 min and stained with aniline blue for 5 min. All these steps were performed at room temperature. The sections were sealed with neutral resin and images were captured using a slide scanning image system (SQS-1000SQS-1000, Shenzhen Shengqiang Technology Co., Ltd.).

Reverse transcription-quantitative PCR (RT-qPCR). Total RNA was extracted from the liver tissues using TRIzol®, and reverse-transcribed into cDNA using the ReverTra Ace qPCR RT kit according to the manufacturer's protocol. qPCR was conducted on a Roche LightCycler 96 real-time PCR system using SYBR-Green as the detection fluorophore (95˚C, 5 sec; 60˚C, 34 sec). The expression of TGF-β1, Smad2, Smad3, Smad7 and α-SMA was normalized to that of the housekeeping gene β-actin. The relative mRNA expression was quantified using the $2^{-\Delta\Delta Cq}$ method (26). The primer sequences used are listed in Table I.

Table I. Primer sequences for reverse transcription-quantitative PCR.

Gene	Sequence (5'-3')
TGF-β1	
Forward	CTCCCGTGGCTTCTAGTGC
Reverse	GCCTTAGTTTGGACAGGATCTG
Smad2	
Forward	ATGTCGTCCATCTTGCCATTC
Reverse	AACCGTCCTGTTTTCTTTAGCTT
Smad3	
Forward	CACGCAGAACGTGAACACC
Reverse	GGCAGTAGATAACGTGAGGGA
Smad7	
Forward	GGCCGGATCTCAGGCATTC
Reverse	TTGGGTATCTGGAGTAAGGAGG
α-SMA	
Forward	GCGTGGCTATTCCTTCGTGACTAC
Reverse	CATCAGGCAGTTCGTAGCTCTTCTC
β-actin	
Forward	CACGATGGAGGGGCCGGACTCATC
Reverse	TAAAGACCTCTATGCCAACAC

α-SMA, α-smooth muscle actin.

Western blotting. A total of 2 ml LX-2 cells were incubated in 6-well plates at a density of $5x10^5$ cells/ml and divided into control, a model (TGF-β1) group and TIIA 20 or 40 μmol/l groups. The control group was treated with complete culture medium, model group with 10 ng/ml TGF-β1 and the TIIA group with either 20 or 40 μmol/l TIIA and 10 ng/ml TGF-β1 by sequential for 24 h. Liver tissues and LX-2 cells were lysed in RIPA lysis buffer and PMSF. The protein concentration was quantified using a BCA protein concentration kit. The proteins (30 μg/lane) were separated by 10% SDS-PAGE Gel Fast Preparation Kit (Epizyme, Inc.). The separated proteins were subsequently transferred to a PVDF membranes, blocked with 5% skimmed milk for 2 h at room temperature, and blotted overnight at 4˚C with primary antibodies. Primary antibodies included TGF-β1 (1:1,000), Smad2/3 (1:1,500), p-Smad2/3 (1:1,500), Smad7 (1:2,500) and α-SMA (1:1,500). β-actin (1:2,500) was used as loading control. Blots were rinsed by TBST buffer (Tween-20, 1%) and the membranes were incubated with a goat anti-rabbit horseradish peroxidase-conjugated IgG secondary antibody (1:500, cat. no. Ab6721; Abcam) at room temperature for 4 h. Following another triple wash, proteins were detected using an ECL reagent (ZenBioScience). The intensities of protein bands were quantified using the ImageJ software (version 1.52; National Institutes of Health).

Cell viability assay. A total of 10^5/ml human LX-2 cells (cat. no. HTX2168) [Otwo Biotech (Shenzhen) Inc.] were cultured in 96-well plates, grown to 80-90% confluence, and pre-treated with 100 μl TIIA solution at 10, 20, 40, 80, 160 or 320 μmol/l for 24 h at 37˚C with 5% CO_2. Subsequently, 20 μl MTS (Promega Corporation) was added to each well, and the plates were further incubated for 1-4 h at 37˚C with 5% CO_2. Absorbance was measured at 490 nm using a Spark 10M multimode reader.

Statistical analysis. Results were analyzed with SPSS version 25.0 (IBM Corp.) and GraphPad Prism version 8.0 software (GraphPad Software, Inc.). Data are presented as the mean ± SD from at least three independent experiments. Differences between multiple groups were determined using one-way ANOVA followed by Bonferroni's post hoc test as appropriate. $P<0.05$ was considered to indicate a statistically significant difference.

Results

Effect of TIIA on body weight and food intake in rats induced by MCD diet. To explore the effect of TIIA on the treatment of NASH-F, Wistar rats were fed a normal or MCD diet for up to 8 weeks and changes in body weight and food intake were observed. The body weight of rats in the NASH-F group was decreased at 2-8 weeks compared with the control group. The body weight of rats in the TIIA group was increased at 2-8 weeks as compared with the NASH-F group (Fig. 1A). The food intake of rats in the control group remained stable during the modeling period, and the food intake of rats in the NASH-F and TIIA groups decreased at 2-8 weeks (Fig. 1B). TIIA treatment increased body weight of MCD-induced NASH-F rats, but there is no difference in its food intake.

TIIA changes liver function indexes in rats with MCD-induced NASH-F. MCD-induced rats developed steatohepatitis similar to NASH-F. NASH-F group had a notable increase in serum ALT and AST (Fig. 2A), which are markers used to indicate liver dysfunction. Interestingly, TIIA treatment suppressed this increase in liver transaminase (ALT and AST) levels observed in the NASH-F group (Fig. 2A). Similarly, NASH-F group had markedly reduced serum TC and TG levels compared with the control group, and both serum lipid markers showed a tendency for increase in the TIIA group compared with the NASH-F group, but there was no statistical significance. (Fig. 2B). Finally, NASH-F group had higher serum TBIL and TBA levels compared with the control group, and the increase in both bile metabolism markers was suppressed by TIIA treatment (Fig. 2C). Collectively, these serum biochemical data suggested that TIIA can improve liver function, blood cholesterol and bile metabolism in MCD-fed rats.

TIIA ameliorates steatosis and liver fibrosis in rats with MCD-induced NASH-F. The livers of the MCD-induced rats had a pale yellow color and increased volume 8 weeks after the start of the MCD diet, compared with the control group (dark red). However, in the TIIA treatment group, the livers were of a mixed yellow and red color (Fig. 3A). H&E staining revealed fat vacuoles and inflammatory cell infiltration in the liver tissue of MCD-induced NASH-F rats compared with control animals. Interestingly, TIIA treatment markedly reduced both the number of fat vacuoles and the level of inflammatory cell infiltration (Fig. 3B). In order to further evaluate the liver fibrosis, Masson's trichrome staining was performed. The results showed hepatic lobule structure disorder, central vein area and collagen fibres accumulated in the NASH-F group. TIIA treatment was associated with improved liver structure, with only a small amount of collagen deposition in the hepatic hilar region (Fig. 3C). In summary, histological analysis showed that TIIA notably reduced the number of fat vacuoles, inflammatory infiltration and fibrosis in NASH-F rats.

TIIA decreases the serum levels of liver fibrosis indicators in rats with MCD-induced NASH-F. To determine whether TIIA can improve liver fibrosis, ELISA was performed to determine whether TIIA can reduce the serum levels of four liver fibrosis indicators in NASH-F rats. Compared with the control group, the serum levels of HA, IV-C, LN and PC-III were markedly elevated in NASH-F group, indicating increased HF. TIIA treatment notably suppressed the serum levels of all four indicators of fibrosis, thereby preventing the increase of fibrosis observed in MCD-fed rats (Fig. 4A-D). Collectively, these data confirmed the beneficial effects of TIIA on liver fibrosis developed in MCD-fed rats.

Effect of TIIA on mRNA expression levels of the TGF-β1/Smad signaling pathway components in rats with MCD-induced NASH-F. To explore whether TIIA can inhibit the progression of fibrosis, qPCR analysis was performed to determine whether TIIA can reduce the expression of TGF-β1, α-SMA, Smad2 and Smad3, and increase the expression of Smad7 in NASH-F rats. The mRNA expression levels of TGF-β1, α-SMA, Smad2 and Smad3 were markedly increased in the livers of NASH-F group compared with the control group and this increase was notably suppressed by TIIA treatment (Fig. 5A-D). The opposite pattern was observed for Smad7, with its mRNA levels being markedly suppressed in the livers of MCD-fed rats compared with control group, which was reversed by TIIA treatment (Fig. 5E).

TIIA modulates protein expression of the TGF-β1/Smad signaling pathway components in rats with MCD-induced NASH-F. To further investigate the effect of TIIA on the TGF-β/Smad signaling pathway, the protein levels of TGF-β1, p-Smad2/3, Smad2/3, Smad7 and α-SMA were examined by western blotting. The protein levels of TGF-β1, p-Smad2/3 and α-SMA were markedly increased in the NASH-F group compared with the control group. TIIA treatment reduced TGF-β1, α-SMA and p-Smad2/3 protein levelscompared with the NASH-F group, similarly to the observations in the mRNA level. The opposite pattern was observed for Smad7, with its protein levels being reduced in the livers of NASH-F rats and this decrease being reversed by TIIA treatment, but there was no statistical significance. (Fig. 6A-E). As the Smad2/3 protein levels remained unchanged, TIIA was associated with both a reduction in p-Smad2/3 and the ratio of p-Smad2/3 to total Smad2/3 compared with the NASH-F group (Fig. 6C-E).

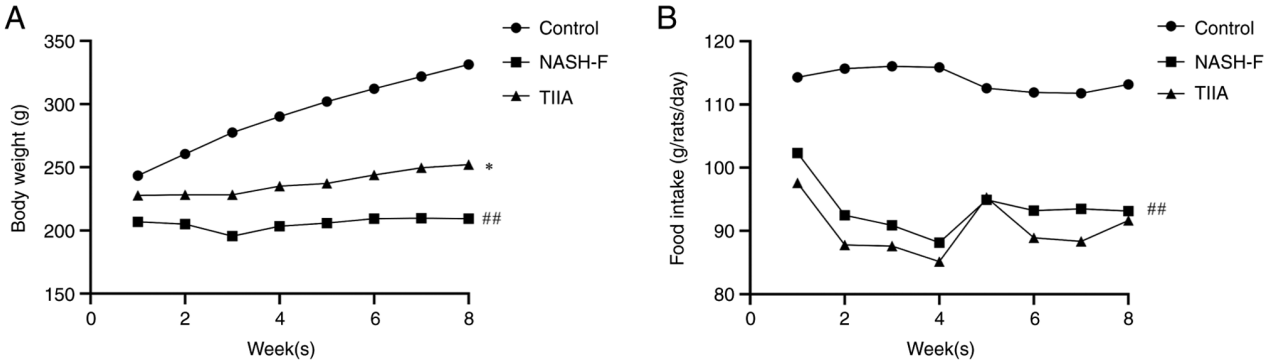

Figure 1. Effects of TIIA on body weight and food intake in methionine choline deficiency diet-induced rats. (A) Weight of NASH-F rats was significantly decreased compared with that of control rats between 2 and 8 weeks. $^{\#\#}$P<0.01 vs. control group (n=8). The weight of TIIA rats was increased between 2 and 8 weeks compared with that of NASH-F rats. *P<0.05 vs. NASH-F group (n=8). (B) Control rats maintained a stable food intake during the modeling period. The food intake of the NASH-F group was decreasedcompared with the control group. $^{\#\#}$P<0.01 vs. control group (n=8). The food intake of the TIIA group decreased compared with the NASH-F group, but there was no statistical significance (P=0.078; n=8). NASH-F, non-alcoholic steatohepatitis-related fibrosis; TIIA, tanshinone IIA.

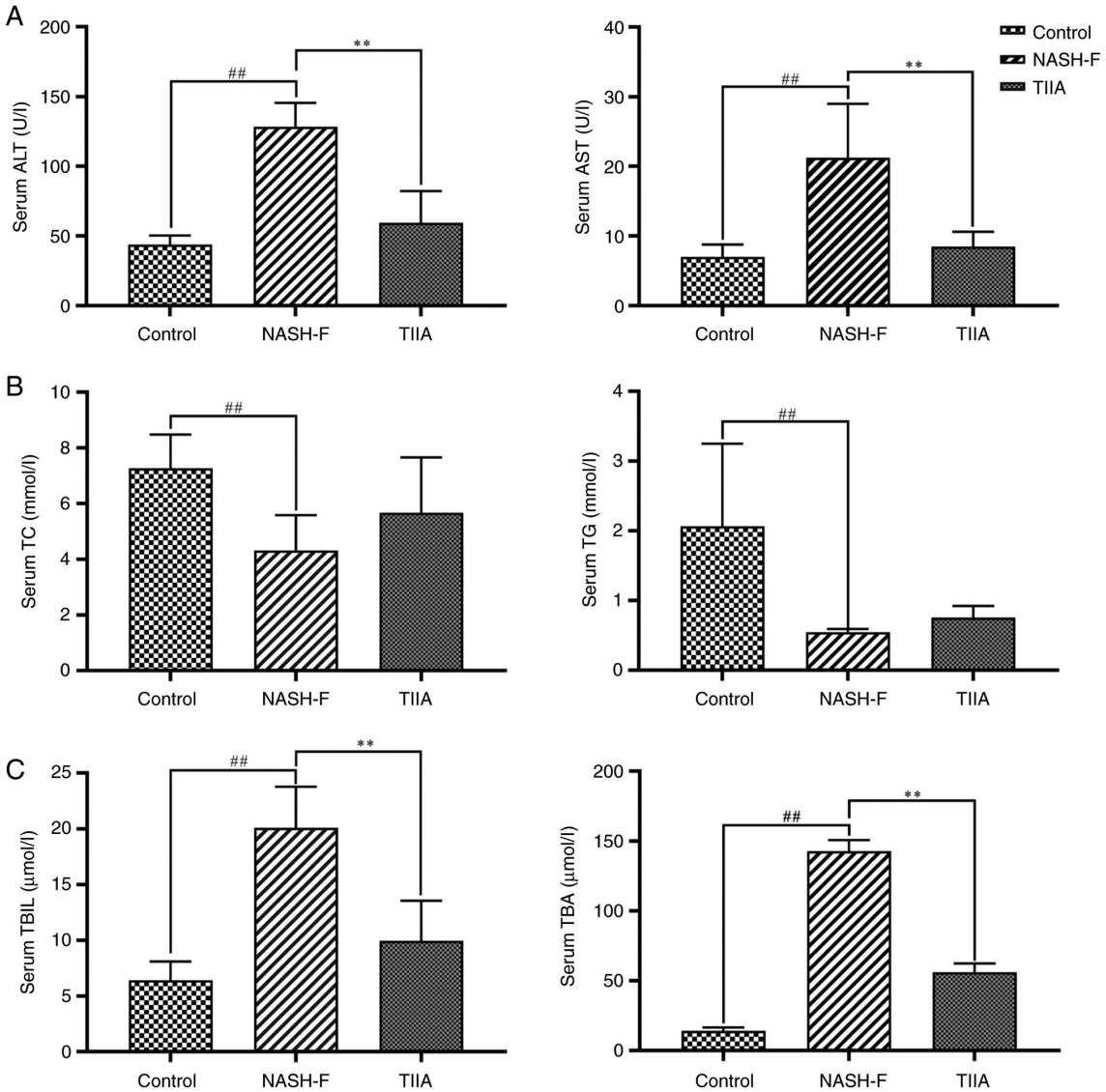

Figure 2. Effects of TIIA on serum transaminase, lipid, TBIL and TBA levels in methionine choline deficiency diet-fed rats. (A) Serum transaminase levels in rats (ALT, NASH-F vs. control, P=0.001; and TIIA vs. NASH-F, P=0.008; AST, NASH-F vs. control, P=0.002; and TIIA vs. NASH-F, P=0.006). (B) Serum lipid levels in rats (TC, NASH-F vs. control, P=0.005; and TIIA vs. NASH-F, P=0.147; TG, NASH-F vs. control, P<0.001; and TIIA vs. NASH-F, P=0.074). (C) Serum TBIL and TBA levels in rats (TBIL, NASH-F vs. control, P<0.001; and TIIA vs. NASH-F, P<0.001; TBA, NASH-F vs. control, P<0.001; and TIIA vs. NASH-F, P=0.004). $^{\#\#}$P<0.01; **P<0.01 (n=6). NASH-F, non-alcoholic steatohepatitis-related fibrosis; TIIA, tanshinone IIA; ALT, alanine aminotransferase; AST, aspartate aminotransferase; TC, total cholesterol; TG, triglycerides; TBIL, total bilirubin; TBA, total bile acid.

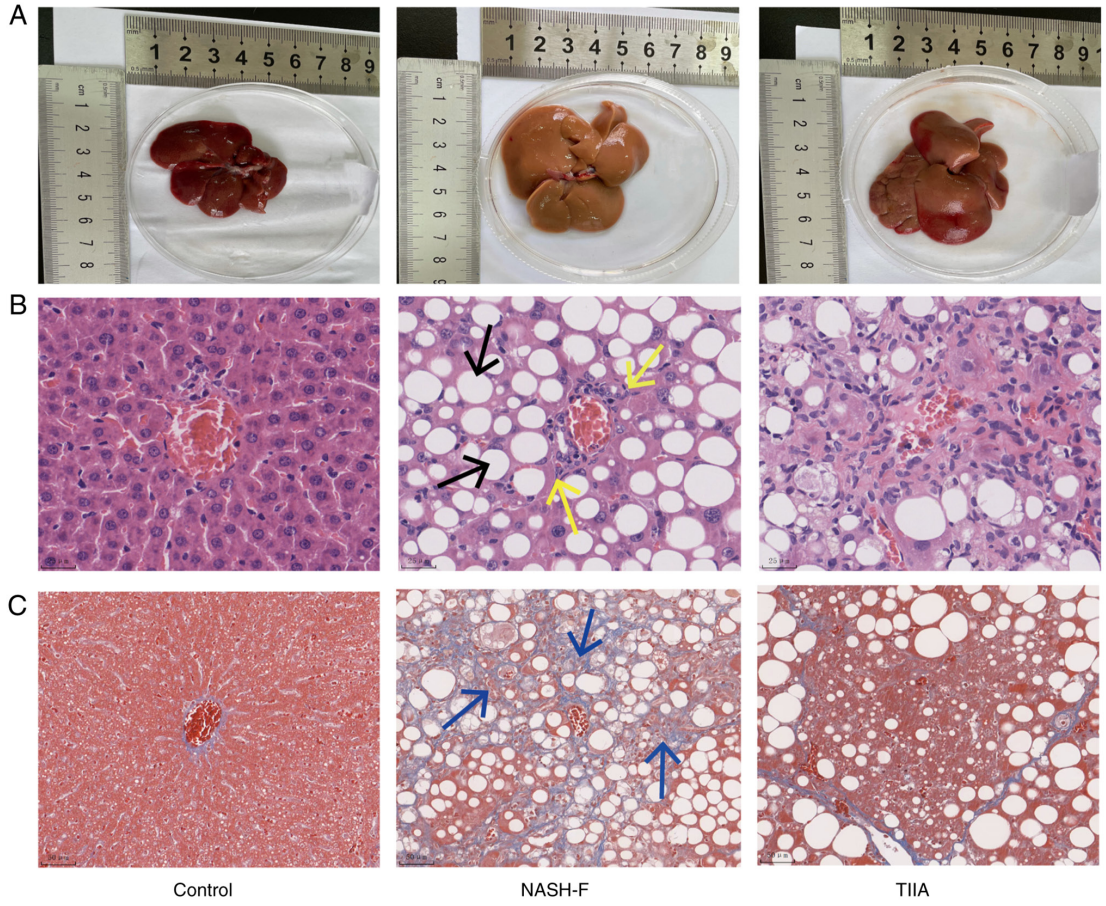

Figure 3. TIIA decreases fat vacuoles, inflammation and fibrosis in methionine choline deficiency diet-induced NASH-F rats. (A) Representative macroscopic images of livers. (B) H&E staining of the liver sections (magnification, x400). The black arrow indicates fat vacuoles, and the yellow arrow indicates inflammatory cell infiltration. (C) Masson's trichrome staining of liver sections from rats (magnification, x200). Blue arrows refer to fibrosis. NASH-F, non-alcoholic steatohepatitis-related fibrosis; TIIA, tanshinone IIA.

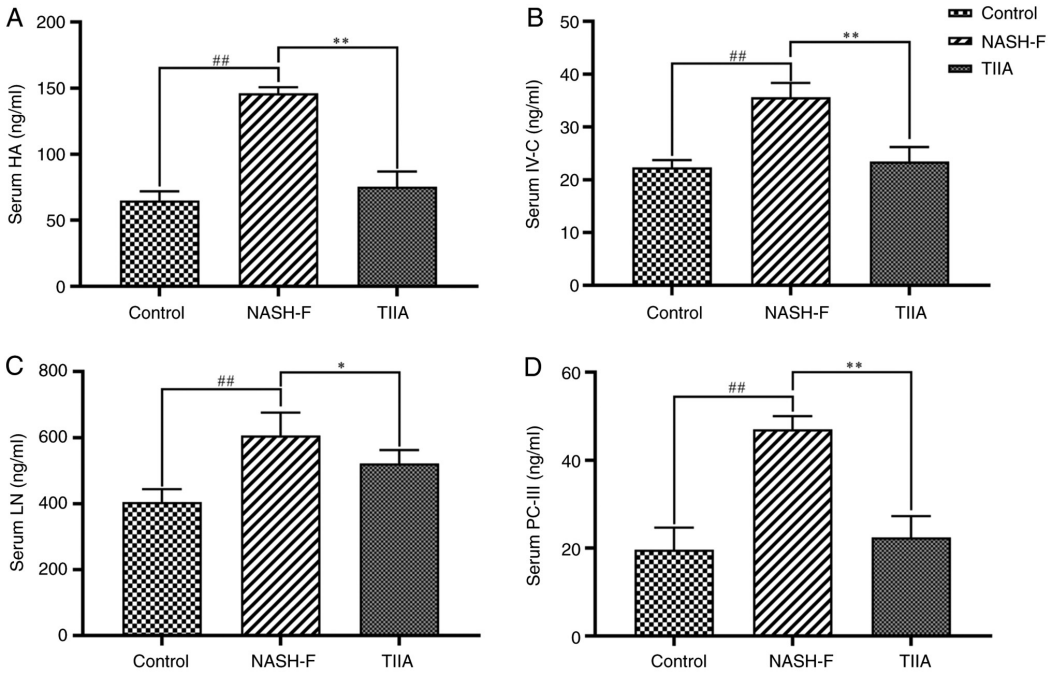

Figure 4. Effects of TIIA on serum levels of four liver fibrosis indicators in methionine choline deficiency diet-fed rats. ELISA analyses of (A) HA (NASH-F vs. control, P<0.001; and TIIA vs. NASH-F, P<0.001), (B) IV-C (NASH-F vs. control, P<0.001; and TIIA vs. NASH-F, P<0.001), (C) LN (NASH-F vs. control, P<0.001; and TIIA vs. NASH-F, P=0.013) and (D) PC-III (NASH-F vs. control, P<0.001; and TIIA vs. NASH-F, P<0.001). $^{\#\#}$P<0.01; *P<0.05; **P<0.01 (n=6). NASH-F, non-alcoholic steatohepatitis-related fibrosis; TIIA, tanshinone IIA; HA, hyaluronic acid; IV-C, type IV collagen; LN, laminin; PC-III, type III collagen.

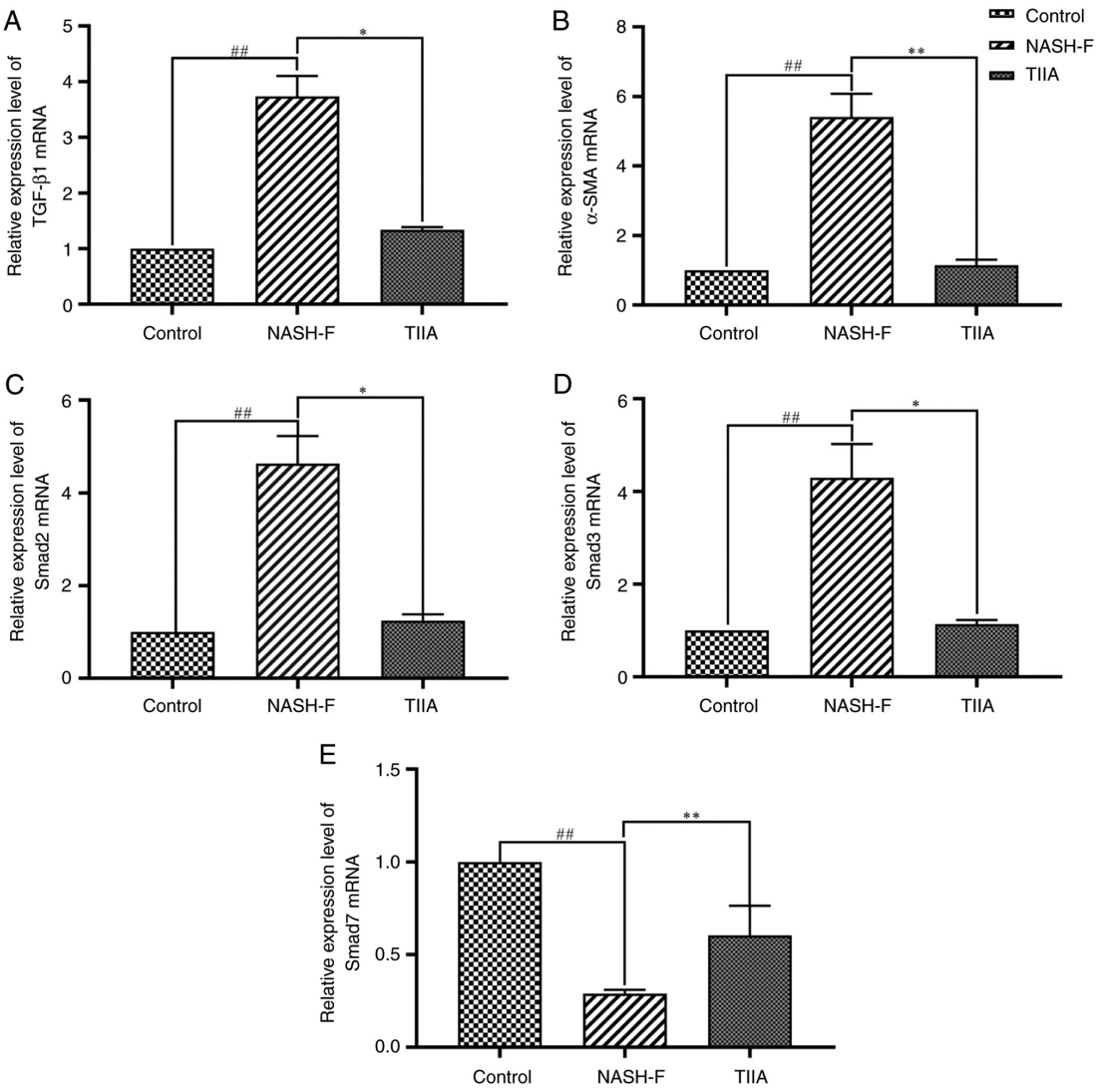

Figure 5. Effects of TIIA on the mRNA levels of the TGF-β1/Smad pathway molecules in methionine choline deficiency diet-fed rats. Reverse transcription-quantitative PCR analyses of (A) TGF-β1 (NASH-F vs. control, P=0.006; and TIIA vs. NASH-F, P=0.024), (B) α-SMA (NASH-F vs. control, P<0.001; and TIIA vs. NASH-F, P<0.001), (C) Smad2 (NASH-F vs. control, P=0.006; and TIIA vs. NASH-F, P=0.024), (D) Smad3 (NASH-F vs. control, P=0.006; and TIIA vs. NASH-F, P=0.024) and (E) Smad7 (NASH-F vs. control, P<0.001; and TIIA vs. NASH-F, P=0.006). $^{\#\#}$P<0.01; *P<0.05; **P<0.01 (n=6). NASH-F, non-alcoholic steatohepatitis-related fibrosis; TIIA, tanshinone IIA; α-SMA, α-smooth muscle actin.

Effect of TIIA on LX-2 cell viability. To study whether TIIA was toxic in LX-2 cells, the effect of different concentrations of TIIA was examined on LX-2 cell viability using MTS. Compared with the control group, 10, 20, 40 and 80 μmol/l TIIA had no effect on cell viability, whereas 160 and 320 μmol/l TIIA significantly reduced the viability of LX-2 cells (Fig. 7). Therefore, concentrations of 20 and 40 μM were selected for subsequent experiments.

TIIA modulates protein expression of the TGF-β1/Smad pathway molecules in the LX-2 cell line. To further investigate the effect of TIIA on the TGF-β1/Smad signaling pathway, the expression levels of α-SMA, Smad2/3, p-Smad2/3 and Smad7 were examined in each group using western blotting. The expression of α-SMA in the model group was significantly increased compared with the control group. Concomitant treatment with TIIA reversed the increase in α-SMA expression induced by TGF-β1. Moreover, as the expression of Smad2/3 remained unchanged, TIIA treatment was associated with a reduction in p-Smad2/3 and the ratio of p-Smad2/3 to total Smad2/3 (Fig. 8A-C). Finally, the reverse pattern was observed for Smad7, with its protein levels being reduced by TGF-β1 and this reduction being reversed by TIIA treatment (Fig. 8D and E). However, there was no difference between the two doses of TIIA.

Discussion

NASH is an important subtype of MAFLD. Its main characteristic is liver inflammation and progressive fibrosis, which eventually damages liver function and the patient's health (27). Liver fibrosis is observed in 37-84% of patients with NASH. thus, HF is the main predictor of progression and death in these patients (28,29). MCD-induced HF in rats is a well-established model of NASH-F, characterized by elevated serum aminotransferase levels and liver histological changes similar to the human NASH-F (30). To explore the effect of TIIA on NASH-F, an MCD diet rat model of HF was used. According to previous research, MCD diet can lead to abnormal liver

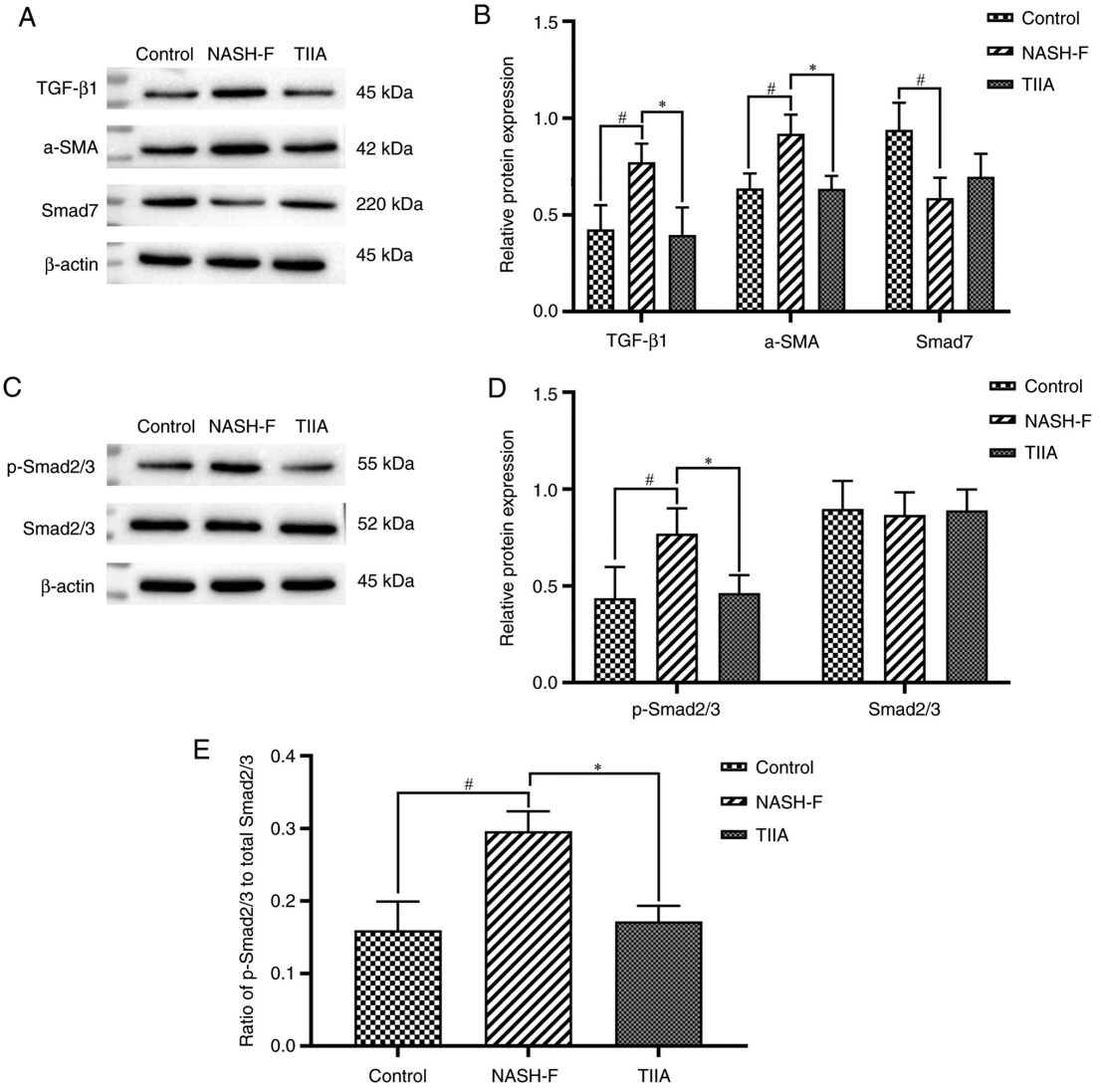

Figure 6. TIIA modulates protein expression of the TGF-β1/Smad pathway molecules. (A) Western blot analysis of TGF-β1, α-SMA and Smad7 protein levels in rat livers. Results were normalized relative to β-actin. (B) Quantification of TGF-β1 (NASH-F vs. control, P=0.013; and TIIA vs. NASH-F, P=0.024), α-SMA (NASH-F vs. control, P=0.019; and TIIA vs. NASH-F, P=0.018) and Smad7 (NASH-F vs. control, P=0.012; and TIIA vs. NASH-F, P=0.300) shown in A. (C) Western blot analysis of p-Smad2/3 and Smad2/3 protein levels in rat livers. Results were normalized relative to β-actin. (D) Quantification of p-Smad2/3 (NASH-F vs. control P=0.049; and TIIA vs. NASH-F, P=0.031) and Smad2/3 (NASH-F vs. control, P=0.776; and TIIA vs. NASH-F, P=0.778) shown in C. (E) Ratio of p-Smad2/3 over total Smad2/3 expression (NASH-F vs. control, P=0.022; and TIIA vs. NASH-F, P=0.022). $^{\#}$P<0.05; *P<0.05 (n=3). NASH-F, non-alcoholic steatohepatitis-related fibrosis; TIIA, tanshinone IIA; p, phosphorylated; α-SMA, α-smooth muscle actin.

metabolism, significant fat accumulation and weight loss (31). In the present study, TIIA treatment could partially prevent the MCD diet-induced weight loss observed in NASH-F rats. Moreover, compared with the NASH-F group, the serum of animals from the TIIA group had lower levels of the liver function (AST, ALT, TBIL, TBA) and liver fibrosis (HA, LN, IV-C, PC-III) indicators and higher levels of TC and TG. These observations, combined with the respective pathology results, indicated that TIIA could markedly improve the degree of MCD-induced NASH-F in rats. The results further indicated that TIIA may reduce liver injury and improve liver function by exerting an anti-fibrotic effect.

HSCs and a small number of portal myofibroblasts are activated in NASH-F, resulting in the production and accumulation of ECM (32). Activation of HSCs can cause an imbalance in ECM synthesis and degradation, and induce collagen accumulation, thereby leading to extensive hyperplasia of the fibrous

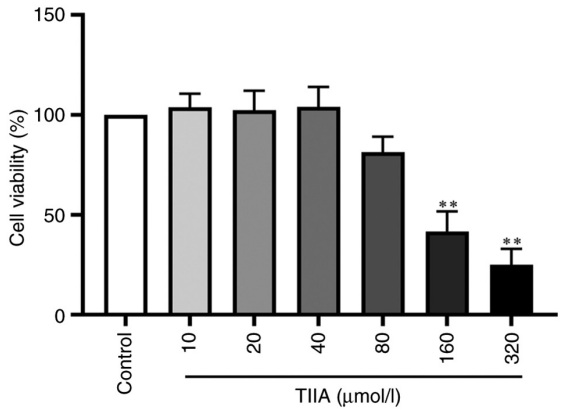

Figure 7. Effects of TIIA on LX-2 cell viability. The viability of LX-2 cells was determined using MTS. TIIA had no significant cytotoxic effect at 10, 20, 40 and 80 μmol/l whereas a significant cytotoxic effect at 160 and 320 μmol/l was observed. **P<0.01 vs. control (n=6). TIIA, tanshinone IIA.

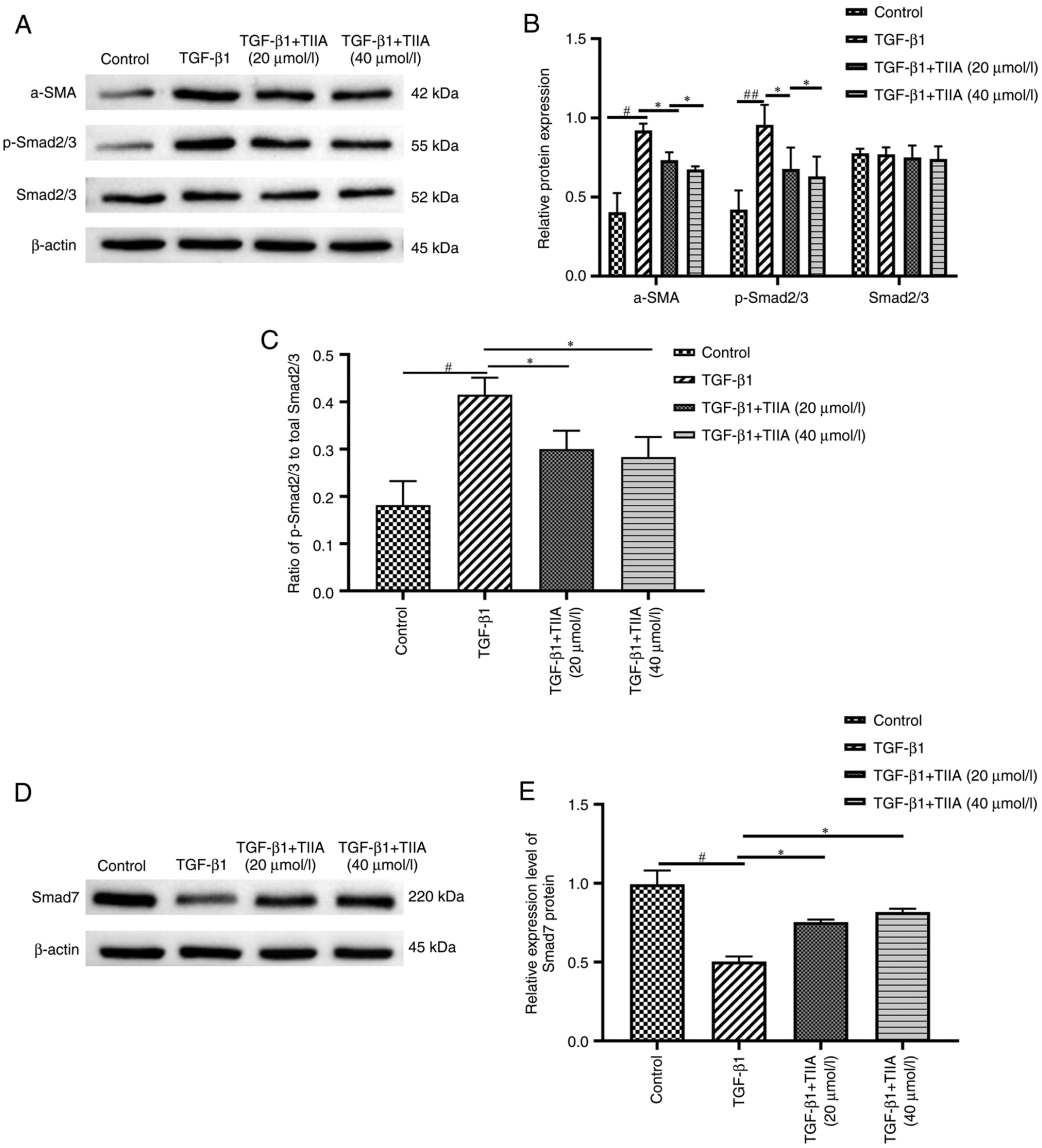

Figure 8. TIIA modulates protein expression of the TGF-β1/Smad pathway molecules *in vitro*. (A) Western blot analysis of α-SMA, p-Smad2/3 and Smad2/3 protein levels in LX-2 cells. Results were normalized relative to β-actin. (B) Quantification of α-SMA [TGF-β1 vs. control, P=0.036; and TIIA vs. TGF-β1, P=0.035 (20 μmol/l) or 0.013 (40 μmol/l), p-Smad2/3 (TGF-β1 vs. control, P=0.001; and TIIA vs. TGF-β1, P=0.027 (20 μmol/l) or 0.014 (40 μmol/l)] and Smad2/3 [TGF-β1 vs. control, P=0.781; and TIIA vs. TGF-β1, P=0.783 (20 μmol/l) or 0.782 (40 μmol/l)] shown in A. (C) Ratio of p-Smad2/3 over total Smad2/3 expression [TGF-β1 vs. control, P=0.035; and TIIA vs. TGF-β1, P=0.025 (20 μmol/l) or 0.015 (40 μmol/l)]. (D) Western blot analysis of Smad7 protein levels in LX-2 cells. Results were normalized relative to expression of β-actin. (E) Quantification of Smad7 expression shown in C [TGF-β1 vs. control, P=0.018; and TIIA vs. TGF-β1, P=0.026 (20 μmol/l) or 0.021 (40 μmol/l)]. $^{\#}$P<0.05; $^{\#\#}$P<0.01; *P<0.05 (n=3). p, phosphorylated; TIIA, tanshinone IIA; α-SMA, α-smooth muscle actin.

tissue as well as high expression of α-SMA protein (33,34). Therefore, HSCs are activated in the resting state and become myofibroblasts, which is a key factor in promoting the development of HF (35). In response to liver injury, HSCs are stimulated to proliferate and are characterized by high expression of α-SMA, which results from TGF-β1-stimulation that is mediated by activated Kupffer cells (36). High α-SMA expression is a typical feature of myofibroblasts, and its induction is the most reliable marker of HSC activation, given that it is absent from other resident liver cells in either normal or damaged liver, except for smooth muscle cells surrounding large vessels (37).

TGF-β/Smad signaling is the classical pathway leading to HSC activation. Upon stimulation with the major TGF subtype (TGF-β1), the TGF-β1 ligand binds to surface receptors on the HSCs, mediating their activation. The Smad2 and Smad3 downstream mediators are then recruited to TGF-β receptors and are activated by phosphorylation (38). Smad2 and Smad3 mainly promote HF, while Smad7 inhibits TGF-β1 signaling, thereby inhibiting HF (39). Specifically, Smad7 is a negative regulatory protein participating in the TGF-β/Smad signaling pathway, which acts in a competitive fashion against TGF-βRI to prevent phosphorylation of Smad2/3, thus inhibiting the activation of the TGF-β/Smad cascade (40). The present study demonstrated that, compared with the NASH-F group, TIIA markedly reduced α-SMA mRNA and protein expression in the rat liver tissue, indicating that TIIA could inhibit the activation of HSCs and reduce the synthesis of ECM, thereby preventing the development of NASH-F. Furthermore, as TGF-β1/Smad signaling is a key pathway leading to HF, the mechanisms via

which TIIA attenuates MCD-induced NASH-F was investigated by examining the TGF-β1/Smad signaling pathway. The results revealed that TIIA notably inhibited the expression of TGF-β1 mRNA and protein levels, decreased the expression of Smad2 and Smad3 mRNA and p-Smad2/3 protein levels, and increased Smad7 mRNA and protein levels in the liver tissue, compared with the NASH-F group. *In vitro* experiments further confirmed the *in vivo* observations. Firstly, the cytotoxicity of different concentrations of TIIA was examined in LX-2 cells and it was revealed that 10, 20, 40 and 80 μmol/l TIIA did not affect the viability of these cells. Subsequently, a cell-based experiment to investigate the effect of TIIA on the TGF-β1/Smad signaling pathway was performed by stimulating LX-2 cells with recombinant human TGF-β1, while at the same time treating the cells with TIIA. The results showed that the effects of TIIA on expression of the TGF-β1/Smad signaling protein were the same both *in vivo* and *in vitro*. Overall, these observations suggested that the TGF-β1/Smad signaling pathway may be involved in the development of NASH-F. The present study investigated the effect of TIIA on TGF-β1/Smad signaling pathway in NASH-F rats without TGF-β antibodies to neutralize bioactivity; this should be included in future research.

In conclusion, the present study investigated the effects of an anti-HF TCM. It also provided convincing evidence demonstrating that TIIA can effectively prevent MCD-induced NASH-F, improve the liver function and prevent the destruction of hepatic tissue and fibrosis progression in a rat model of HF. Finally, the present study demonstrated that TIIA exerted its effects by downregulating the expression of TGF-β1 and p-Smad2/3 and by increasing the expression of Smad7. These observations suggested that TIIA may be useful in inhibiting or reversing progression of NASH-F, and may offer the possibility of developing a novel therapeutic drug for the treatment of chronic liver diseases.

Acknowledgements

Not applicable.

Funding

This work was supported by the National Natural Science Foundation of China (grant nos. 81960814, 81760818 and 82160898), Science and Technology Program of Yunnan Science and Technology Department [grant nos. 2018FF001(-006), 2019FF002(-079) and 202101AZ070001-042] and Yunnan Provincial Key Laboratory of Molecular Biology for Sinomedicine (Yunnan University of Traditional Chinese Medicine; grant no. 2019DG016).

Availability of data and materials

The datasets used and/or analyzed during the current study are available from the corresponding author on reasonable request.

Authors' contributions

LX conceived the study and wrote the manuscript. LX, YZ, NJ and YD carried out the animal model construction and all the animal experiments. LX, TJ, SW and WW acquired, analyzed and interpreted the data and revised the final manuscript. SZ and WC made substantial contributions to the conception and design of the study. LX and SZ confirm the authenticity of all the raw data. All authors have read and approved the final manuscript.

Ethics approval and consent to participate

The animal experiments of the current study were approved by the Experimental Animal Ethics Committee of Yunnan University of Traditional Chinese Medicine (Kunming, China; approval no. R-062021021).

Patient consent for publication

Not applicable.

Competing interests

The authors declare that they have no competing interests.

References

1. Eslam M, Newsome PN, Sarin SK, Anstee QM, Targher G, Romero-Gomez M, Zelber-Sagi S, Wai-Sun Wong V, Dufour JF, Schattenberg JM, *et al*: A new definition for metabolic dysfunction-associated fatty liver disease: An international expert consensus statement. J Hepatol 73: 202-209, 2020.
2. Arab JP, Arrese M and Trauner M: Recent insights into the pathogenesis of nonalcoholic fatty liver disease. Annu Rev Pathol 13: 321-350, 2018.
3. Powell EE, Wong VW and Rinella M: Non-alcoholic fatty liver disease. Lancet 397: 2212-2224, 2021.
4. Thibaut R, Gage MC, Pineda-Torra I, Chabrier G, Venteclef N and Alzaid F: Liver macrophages and inflammation in physiology and physiopathology of non-alcoholic fatty liver disease. FEBS J: Apr 15, 2021 (Epub ahead of print).
5. Zhang CY, Yuan WG, He P, Lei JH and Wang CX: Liver fibrosis and hepatic stellate cells: Etiology, pathological hallmarks and therapeutic targets. World J Gastroenterol 22: 10512-10522, 2016.
6. Zhang Y, Miao H, Yan H, Sheng Y and Ji L: Hepatoprotective effect of forsythiae fructus water extract against carbon tetrachloride-induced liver fibrosis in mice. J Ethnopharmacol 218: 27-34, 2018.
7. Liu J, Kong D, Qiu J, Xie Y, Lu Z, Zhou C, Liu X, Zhang R and Wang Y: Praziquantel ameliorates CCl_4-induced liver fibrosis in mice by inhibiting TGF-β/Smad signalling via up-regulating Smad7 in hepatic stellate cells. Br J Pharmacol 176: 4666-4680, 2019.
8. Walton KL, Johnson KE and Harrison CA: Targeting TGF-β mediated SMAD signaling for the prevention of fibrosis. Front Pharmacol 8: 461, 2017.
9. Karin D, Koyama Y, Brenner D and Kisseleva T: The characteristics of activated portal fibroblasts/myofibroblasts in liver fibrosis. Differentiation 92: 84-92, 2016.
10. Massagué J: TGF-β signalling in context. Nat Rev Mol Cell Biol 13: 616-130, 2012.
11. Fabregat I, Moreno-Càceres J, Sánchez A, Dooley S, Dewidar B, Giannelli G and Ten Dijke P; IT-LIVER Consortium: TGF-β signalling and liver disease. FEBS J 283: 2219-2232, 2016.
12. Giannelli G, Mikulits W, Dooley S, Fabregat I, Moustakas A, Ten Dijke P, Portincasa P, Winter P, Janssen R, Leporatti S, *et al*: The rationale for targeting TGF-β in chronic liver diseases. Eur J Clin Invest 46: 349-361, 2016.
13. Yan C, Wang L, Li B, Zhang BB, Zhang B, Wang YH, Li XY, Chen JX, Tang RX and Zheng KY: The expression dynamics of transforming growth factor-β/Smad signaling in the liver fibrosis experimentally caused by clonorchis sinensis. Parasit Vectors 8: 70, 2015.
14. Li B, Yan C, Wu J, Stephane K, Dong X, Zhang YZ, Zhang Y, Yu Q and Zheng KY: Clonorchis sinensis ESPs enhance the activation of hepatic stellate cells by a cross-talk of TLR4 and TGF-β/Smads signaling pathway. Acta Trop 205: 105307, 2020.

15. El Nashar EM, Alghamdi MA, Alasmari WA, Hussein MMA, Hamza E, Taha RI, Ahmed MM, Al-Khater KM and Abdelfattah-Hassan A: Autophagy promotes the survival of adipose mesenchymal stem/stromal cells and enhances their therapeutic effects in cisplatin-induced liver injury via modulating TGF-β1/Smad and PI3K/AKT signaling pathways. Cells 10: 2475, 2021.
16. Dooley S, Hamzavi J, Breitkopf K, Wiercinska E, Said H, Lorenzen J, Ten Dijke P and Gressner AM: Smad7 prevents activation of hepatic stellate cells and liver fibrosis in rats. Gastroenterology 125: 178-191, 2003.
17. Choi JH, Jin SW, Choi CY, Kim HG, Lee GH, Kim YA, Chung YC and Jeong HG: Capsaicin inhibits dimethylnitrosamine-induced hepatic fibrosis by inhibiting the TGF-β1/Smad pathway via peroxisome proliferator-activated receptor gamma activation. J Agric Food Chem 65: 317-326, 2017.
18. Bai G, Yan G, Wang G, Wan P and Zhang R: Anti-hepatic fibrosis effects of a novel turtle shell decoction by inhibiting hepatic stellate cell proliferation and blocking TGF-β1/Smad signaling pathway in rats. Oncol Rep 36: 2902-2910, 2016.
19. Peng Y, Yang T, Huang K, Shen L, Tao Y and Liu C: *Salvia miltiorrhiza* ameliorates liver fibrosis by activating hepatic natural killer cells in vivo and in vitro. Front Pharmaco 9: 762, 2018.
20. Yan Q, Mao Z, Hong J, Gao K, Niimi M, Mitsui T and Yao J: Tanshinone IIA stimulates cystathionine γ-lyase expression and protects endothelial cells from oxidative injury. Antioxidants (Basel) 10: 1007, 2021.
21. Chen Z, Gao X, Jiao Y, Qiu Y, Wang A, Yu M, Che F, Li S, Liu J, Li J, *et al*: Tanshinone IIA exerts anti-inflammatory and immune-regulating effects on vulnerable atherosclerotic plaque partially via the TLR4/MyD88/NF-κB signal pathway. Front Pharmacol 10: 850, 2019.
22. Subedi L and Gaire BP: Tanshinone IIA: A phytochemical as a promising drug candidate for neurodegenerative diseases. Pharmacol Res 169: 105661, 2021.
23. Bi Z, Wang Y and Zhang W: A comprehensive review of tanshinone IIA and its derivatives in fibrosis treatment. Biomed Pharmacother 137: 111404, 2021.
24. Shi MJ, Yan XL, Dong BS, Yang WN, Su SB and Zhang H: A network pharmacology approach to investigating the mechanism of Tanshinone IIA for the treatment of liver fibrosis. J Ethnopharmacol 253: 112689, 2020.
25. Sun X, Tan Y, Lyu J, Liu HL, Zhao ZM and Liu CH: Active components formulation developed from fuzheng huayu recipe for anti-liver fibrosis. Chin J Integr Med: Sep 28, 2021 (Epub ahead of print).
26. Livak KJ and Schmittgen TD: Analysis of relative gene expression data using real-time quantitative PCR and the 2(-Delta Delta C(T)) method. Methods 25: 402-408, 2001.
27. Chalasani N, Younossi Z, Lavine JE, Charlton M, Cusi K, Rinella M, Harrison SA, Brunt EM and Sanyal AJ: The diagnosis and management of nonalcoholic fatty liver disease: Practice guidance from the American association for the study of liver diseases. Hepatology 67: 328-357, 2018.
28. Wong VW, Wong GL, Choi PC, Chan AW, Li MK, Chan HY, Chim AM, Yu J, Sung JJ and Chan HL: Disease progression of non-alcoholic fatty liver disease: A prospective study with paired liver biopsies at 3 years. Gut 59: 969-974, 2010.
29. Taylor RS, Taylor RJ, Bayliss S, Hagström H, Nasr P, Schattenberg JM, Ishigami M, Toyoda H, Wai-Sun Wong V, Peleg N, *et al*: Association between fibrosis stage and outcomes of patients with nonalcoholic fatty liver disease: A systematic review and meta-analysis. Gastroenterology 158: 1611-1625.e12, 2020.
30. Li R, Li J, Huang Y, Li J, Yan S, Lin J, Chen Y, Wu L, Liu B, Wang G and Lan T: Polydatin attenuates diet-induced nonalcoholic steatohepatitis and fibrosis in mice. Int J Biol Sci 14: 1411-1425, 2018.
31. Li X, Wang TX, Huang X, Li Y, Sun T, Zang S, Guan KL, Xiong Y, Liu J and Yuan HX: Targeting ferroptosis alleviates methionine-choline deficient (MCD)-diet induced NASH by suppressing liver lipotoxicity. Liver Int 40: 1378-1394, 2020.
32. Zisser A, Ipsen DH and Tveden-Nyborg P: Hepatic stellate cell activation and inactivation in NASH-fibrosis-roles as putative treatment targets? Biomedicines 9: 365, 2021.
33. Czaja AJ: Hepatic inflammation and progressive liver fibrosis in chronic liver disease. World J Gastroenterol 20: 2515-2532, 2014.
34. Eom YW, Shim K and Baik SK: Mesenchymal stem cell therapy for liver fibrosis. Korean J Intern Med 30: 580-589, 2015.
35. Seki E and Brenner DA: Recent advancement of molecular mechanisms of liver fibrosis. J Hepatobiliary Pancreat Sci 22: 512-518, 2015.
36. Xu S, Mao Y, Wu J, Feng J, Li J, Wu L, Yu Q, Zhou Y, Zhang J, Chen J: TGF-β/Smad and JAK/STAT pathways are involved in the anti-fibrotic effects of propylene glycol alginate sodium sulphate on hepatic fibrosis. J Cell Mol Med 24: 5224-5237, 2020.
37. Friedman SL: Hepatic stellate cells: Protean, multifunctional, and enigmatic cells of the liver. Physiol Rev 88: 125-172, 2008.
38. Li Z, Wang Z, Dong F, Shi W, Dai W, Zhao J, Li Q, Fang ZE, Ren L, Liu T, *et al*: Germacrone attenuates hepatic stellate cells activation and liver fibrosis via regulating multiple signaling pathways. Front Pharmacol 12: 745561, 2021.
39. Yu K, Li Q, Shi G and Li N: Involvement of epithelial-mesenchymal transition in liver fibrosis. Saudi J Gastroenterol 24: 5-11, 2018.
40. Zhou QY, Yang HM, Liu JX, Xu N, Li J, Shen LP, Zhang YZ, Koda S, Zhang BB, Yu Q, *et al*: MicroRNA-497 induced by clonorchis sinensis enhances the TGF-β/Smad signaling pathway to promote hepatic fibrosis by targeting Smad7. Parasit Vectors 14: 472, 2021.